Electron-impact energy dependence of the sodium K-shell double-ionization cross section: A study of hypersatellite spectra

J. Auerhammer, H. Genz, G. Kilgus, A. Kumar,* and A. Richter
Institut für Kernphysik, Technische Hochschule Darmstadt, 6100 Darmstadt, West Germany
(Received 29 December 1986)

The $K\alpha_2^h$ (L^{-n}; $n=0-5$) hypersatellite spectrum of sodium has been detected for various electron-impact energies in the range of $15 \leq E_0 \leq 200$ keV. The measured energies of the transitions are in agreement with results of previous experiments at low electron energies and theoretical predictions. For the strongest hypersatellite, which corresponds to a $K^{-2} \rightarrow K^{-1}L^{-1}$ transition, the natural width has been determined. The natural linewidth was found to be $\Gamma_K^h = 2.2 \pm 0.4$ eV, which is much larger than predicted. Furthermore, the electron double-ionization cross section of the K shell has been obtained. Within the investigated energy region the cross section decreases by about a factor of 4 with increasing electron-impact energy. This energy dependence suggests the dominance of direct double ionization in comparison to the shake-off process.

I. INTRODUCTION

In recent years thorough investigations have been performed to study electron-induced single K-shell ionization processes and they have considerably improved our understanding of the excitation mechanism in the electron-atom scattering. Only little information has become available about the simultaneous creation of a K- and an L-shell vacancy and nearly none on the electron double-ionization cross section of the K shell where, in addition, information regarding the coupling scheme and the multiple excitation mechanism are furnished. Due to the rather small probability of occurrence of the initial K^{-2}-state configuration during the excitation process of an atom, the experimental investigations on the decay of double vacancies are scarce in the literature.[1-5] The study of the process requires spectroscopy of the $K\alpha$ hypersatellites which arise as a result of a $1s^{-1} \rightarrow 2p^{-1}$ single-electron intermediate deexcitation of the initial $1s^{-2}$ state configuration. The study on the hypersatellite furnishes information regarding the collision mechanism; the coupling schemes of the two vacancies; the energies, intensities, and decay widths of the various transitions involved; and about the atomic cloud nucleus interaction.[6-10]

It has been the purpose of the present work to study the energy dependence of the K-shell double-ionization cross section for electron-impact energies ranging up to the relativistic region. Such a detailed study of this process might serve as a first tool in formulating a model that describes the multiple-excitation mechanism of the simplest K^{-2} state. This is an interesting state in the sense that it is not possible to produce the double K vacancies by cascade transitions and only to a small probability by the shake-off process. Since the decay of the K^{-2} state is also of general interest, we chose sodium as one of the simplest systems where all possible couplings between the K and L shells can be studied. Finally, the present work also checks the validity of a recently deduced empirical law which apparently describes the broadening of the natural linewidth observed in $K^{-2} \rightarrow K^{-1}L^{-1}$ transitions.

Lahtinen and Keski-Rahkonen[11] also studied the electron-induced hypersatellite spectrum of sodium and determined the dependence of the K-shell double-ionization cross section on the electron-impact energy in the region $4 \leq E_0 \leq 25$ keV using thin and thick targets. Their measured value of the double-ionization cross section is at variance with theoretical predictions.[12,13]

The present work reports on the measurement of the energy dependence of the K-shell electron double-ionization cross section in sodium for a wide range of electron energies $15 \leq E_0 \leq 200$ keV (Sec. II). A thorough investigation is made of the intensities and energies of the hypersatellites ($K^{-2}L^{-0} \rightarrow K^{-1}L^{-1}$) and the satellites of hypersatellites ($K^{-2}L^{-1} \rightarrow K^{-1}L^{-2}$; $K^{-2}L^{-2} \rightarrow K^{-1}L^{-3}$; ...; etc.). Also, the natural width of the hypersatellite line is measured in view of the lifetime of the K^{-2} state (Sec. III). All results are discussed in Sec. IV.

II. EXPERIMENTAL METHOD

The experiment was performed at our superconducting pilot accelerator facility[14] and since the whole setup is described in detail elsewhere,[15,16] we will focus here only on a few important aspects. The experimental arrangement is displayed in Fig. 1. Electrons from an electron gun were focused over a distance of about 2 m onto the target and were collected in a Faraday cup. A vacuum of nearly 10^{-7} Torr was maintained near the electron gun and of approximately 10^{-6} Torr in the vicinity of the target. Thin targets of sodium fluoride (NaF) were prepared under a high vacuum (10^{-6} Torr) on carbon substrate (10 μg/cm^2) by an evaporation technique. The target (NaF) thickness was measured to be 160 μg/cm^2 using the method of the energy loss of α particles. The target size amounted to about 80 mm^2, and the electron beam impinged on a circular area of about 5 mm diameter.

The emitted characteristic x-ray radiation from the target was studied perpendicular to the beam axis ($\theta = 90°$) employing a high-resolution flat crystal Bragg spectrometer equipped with a thallium acid phthalate (TlAP) crystal ($2d = 25.745$ Å). The target-spectrometer distance was maintained to 100 cm to reduce the scattered background

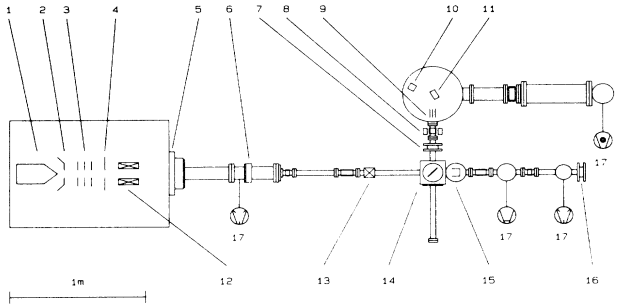

FIG. 1. Experimental setup: 1 denotes cathode; 2—4, potential grids; 5, lens; 6,7,16, vacuum valves; 8, deflecting magnet; 9, Soller slits; 10, x-ray detector; 11, Bragg crystal; 12,13, horizontal and vertical steerer; 14, target chamber; and 15, Faraday cup.

radiation. A strong magnetic field (800 G) deflected scattered electrons from the radiation path. Finally, a long Soller slit of dimension $20\times30\times150$ mm^3 was placed in the radiation path. The slit width amounted to 0.1 mm which gave a divergence angle of 0.076° from the target. The present setup had the advantage of a low background radiation which enhanced the signal-to-background ratio. This has been crucial to the present measurement since a high background could have easily suppressed the weak signals from hypersatellite transitions.

The characteristic x-ray radiation was diffracted from the TlAP crystal, and then detected by a flow gas proportional counter operated at a pressure of 760 Torr using a gas mixture of argon (90%) and methane (10%). A Mylar window coated with aluminum (2 μg/cm^2) separated the proportional counter from the vacuum of the spectrometer.

The spectra were observed with a step scanning method. At each Bragg angle the x-ray intensity was measured for a definite charge (e.g., 50 μC) determined by integrating the incident electron flux using a Faraday cup. The intensity of x-ray radiation was collected with an increment of $\Delta\theta=2\times10^{-2}$ degrees Bragg angle. A computer-controlled scanning procedure furnished the x-ray intensities as a function of angle. All functions concerning the setting of the crystal and the detector, the charge registered per step, step sizes and intervals, number of sweeps needed to obtain sufficient statistics, and the data acquisition were controlled by an LSI 11/23 computer. Finally, a DEC Vax 11/750 computer served for data analysis. For calibration of the spectrometer we used the position of the Na $K\alpha_{1,2}$ line which could be reproduced with an accuracy of ±0.11 eV. Once this was accomplished, the spectrometer was set to scan the spectrum around the hypersatellite lines and subsequently again around the $K\alpha$ position. The $K\alpha$ spectra and the hypersatellites of sodium were measured at 15-, 25-, 50-, 100-, 150-, and 200-keV electron-impact energies.

III. ANALYSIS AND RESULTS

A typical Na $K\alpha$ spectrum is shown in the upper part of Fig. 2. The largest peak is due to a pure $K\alpha$ ($1s^{-1}\rightarrow2p^{-1}_{1/2,3/2}$) transition with no vacancy in the L shell in the initial-state configuration. On the higher-energy side of this peak several structures were noticed which are attributed to multiple vacancies in the L shell. The spectra were analyzed applying a fitting procedure that has successfully been employed previously.[15,16] For the $K\alpha$ line (A) and its satellites (B,C,D) a combination of a Gaussian and a Breit-Wigner function yielded the best fit to the data points as indicated in the lower part of Fig. 2. During the fitting procedure the parameters as peak position and intensity were left variable while the shape of the line, i.e., the full width at half maximum (FWHM), line asymmetry, and the Gaussian to Breit-Wigner ratio were assumed to be the same for all lines. The solid line in the upper part of the figure represents the sum of the fits to the diagram and satellite lines. The intensities and the energies of these peaks were found to be in accordance with previous measurements.[17,18] Since the energy difference of the $K\alpha_1$ and $K\alpha_2$ transition is quite small (<1 eV), it was not possible to resolve these two lines. The energy of the $K\alpha_{1,2}$ transition is observed to be $E(K\alpha)=1041.19\pm0.11$ eV which compares fairly well with the available Dirac-Fock calculated value[17]

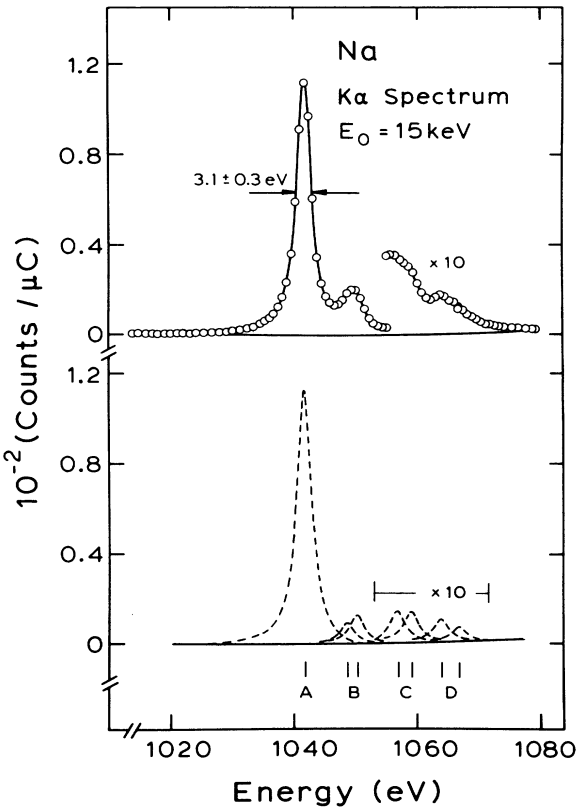

FIG. 2. Sodium $K\alpha$ spectrum obtained by bombarding a thin (160 μg/cm^2) NaF target on a carbon layer with electrons of 15 keV using a flat TlAP crystal (upper part). The lower part displays the result of a fit to the individual lines. The letters A through D characterize the diagram (A) as well as the KL^{-n} satellite lines. The solid line in the upper part of the figure is the sum of the individual lines.

(1042.0 eV) and another similar experiment[17] (1040.9±0.2 eV).

In Fig. 3 the hypersatellite spectra recorded at 15-, 25-, 50-, 100-, 150-, and 200-keV electron-impact energies are displayed. While the recording of a $K\alpha$ spectrum took 3—4 sweeps (40 min) in the desired energy range for a precise measurement of intensity and energy, the $K\alpha$ hypersatellite spectra needed some 600—700 sweeps ($\sim$110—130 h). It is due to the small probability of the $K\alpha^h$ transition relative to the $K\alpha_{1,2}$ transition ($\sim 10^{-4}$). The different spectra have been accumulated for different charges of electrons that have traversed the target. Several lines sitting on a more or less strong background are observed. The most intense line at $E=1146$ eV shows up clearly in all six spectra and most distinctly in the spectrum obtained for a bombarding energy of 15 keV. The peak to background ratio for this line is decreasing with the bombarding energy since the line intensity is decreasing and the background is simultaneously increasing.

A somewhat different fitting procedure than described above was employed in order to deduce the peak energies and intensities unambiguously. First, the spectra were smoothed by always averaging five adjacent data points and moving this "five-data-point" window point by point over the entire spectrum. Two typical examples are displayed in Fig. 4. It shows the smoothed and background-subtracted 15-keV spectrum, which has the best statistics, and the 50-keV spectrum, as a typical example of a spectrum with less pronounced peaks. Then, in contrast to the fitting procedure adopted for the separation of the diagram and satellite lines, a Gaussian shape was assumed for the hypersatellite lines. This was necessary because of the low statistics in the hypersatellite spectra. While the line shapes were assumed to be the same for all lines, positions and intensities of the lines (E—L) were kept variable during the fitting procedure. The results are displayed in the lower part of Fig. 4. The solid lines in the upper part of the figure represent again the sum of the individual fits to E through L.

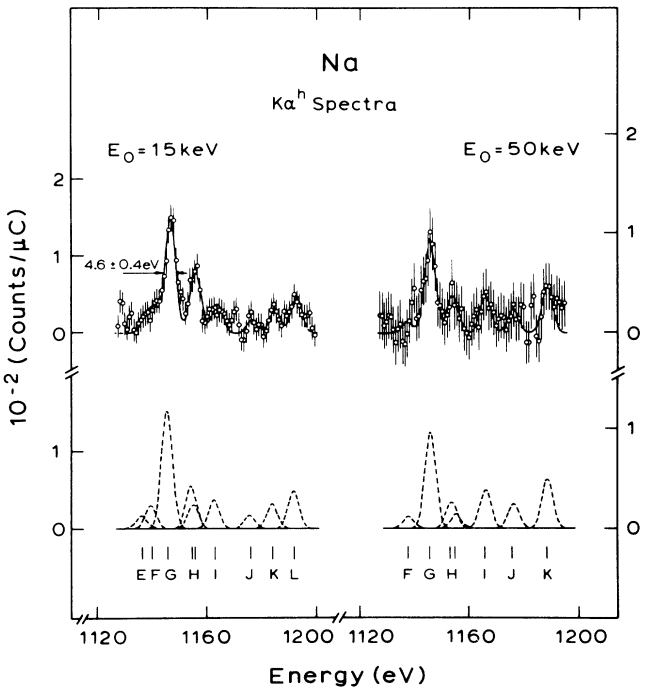

FIG. 4. Sodium hypersatellite spectrum for $E_0=15$ and 25 keV. The spectra are background subtracted and were smoothed according to the procedure described in the main text (upper part). The lower part displays the result of a computer fit to individual lines marked E through L. The sum of these lines are the solid curves shown in the upper part of the figure. Line G designates the investigated $K\alpha_2^h$ hypersatellite.

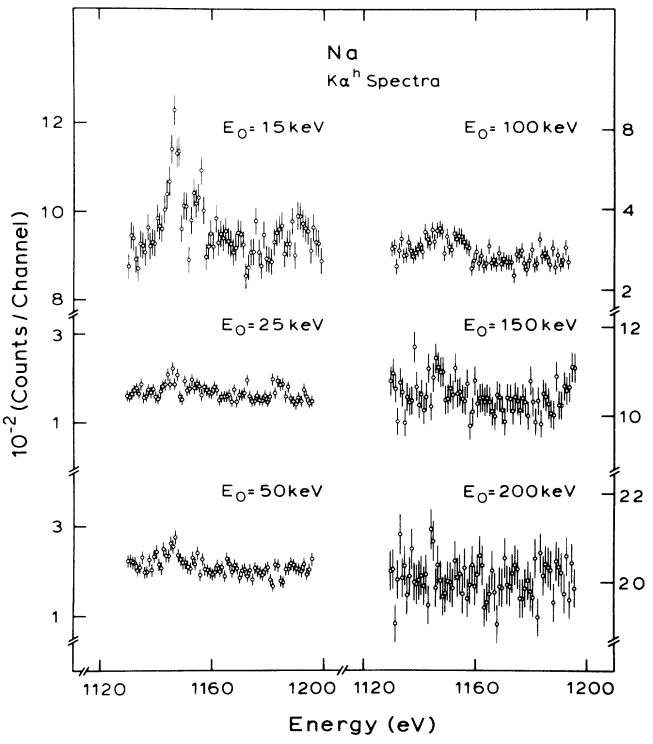

FIG. 3. The sodium hypersatellite spectra obtained for the same conditions as described in Fig. 2 but for all impact electron energies employed.

The energies of the lines measured in the region of the hypersatellite spectrum are compiled in Table I. The reported energy values are the difference of the observed hypersatellite energies with respect to the $K\alpha_{1,2}$ transition energy. They have been obtained by means of the above-described computer fit to the spectrum. The quoted uncertainties in the energy positions of the peaks E—L depict the mean standard deviation of the measured $K\alpha_2^h$ transition energies at various impact energies. Table I also includes the results of the previous measurements for the designated peaks using electron excitation[11] and heavy-ion collision.[17] The last two columns of Table I contain averaged group energies of the designated transitions[17] using the Hartree-Fock program of Froese-Fischer[19] and the Dirac-Fock program of Desclaux,[20] respectively.

TABLE I. Energies of the designated spectral lines of sodium relative to the $K\alpha_{1,2}$ line (1041.19±0.11 eV) in eV as obtained from a fit to the six spectra of Fig. 3.

	Designated transition		Experiment			Theory	
			Present work	Ref. 11	Ref. 17	HF[a]	DF[b]
E			96.6±0.5				
F			99.3±0.8				
G	$K^{-2}\rightarrow K^{-1}L^{-1},K\alpha_2^h(L^0)$		104.5±0.6	104.3±0.1	104.1±0.5	103.3	104.8
H							
		$^2P\rightarrow{}^2P$	112.1±0.9	112.3±0.3		112.7[c]	113.6
	$K^{-2}L^{-1}\rightarrow K^{-1}L^{-2},K\alpha_2^h(L^{-1})$				113.6±0.5		
		$^2P\rightarrow{}^2D$	113.6±1.1	113.5±0.5		113.8[c]	114.5
I	$K^{-2}L^{-2}\rightarrow K^{-1}L^{-3},K\alpha_2^h(L^{-2})$		121.8±2.4		122.8±0.5	119.9	121.2
J	$K^{-2}L^{-3}\rightarrow K^{-1}L^{-4},K\alpha_2^h(L^{-3})$		133.7±1.9		133.8±0.5	131.7	133.1
K	$K^{-2}L^{-4}\rightarrow K^{-1}L^{-5},K\alpha_2^h(L^{-4})$		143.6±2.7		144.3±0.7	146.0	147.4
L	$K^{-2}L^{-5}\rightarrow K^{-1}L^{-6},K\alpha_2^h(L^{-5})$		150.2±2.0		155.3±0.6	160.8	162.5

[a]Hartree-Fock calculation, Ref. 17.
[b]Dirac-Fock calculation, Ref. 17.
[c]From Ref. 11.

Apart from the hypersatellite ($K\alpha_2^h$) and its satellites ($K\alpha_s^h$)—designated by *G* and *H* through *L*, respectively—a few more quite weak transitions were recorded. Two such transitions (*E*,*F*) are shown in Fig. 4 and are compiled in Table I. Four more weak lines were observed at energies 1115, 1122, 1127, and 1134 eV (not shown in Fig. 4). A proper designation for the transitions leading to these lines could not be made. These lines could possibly be due to higher $K\alpha$ or $K\beta$ satellites. This seems plausible since the $K\beta(L^{-2})$ and $K\beta(L^{-3})$ group energies fall quite close to the observed values (1114.7 and 1137.0 eV, respectively).[17] The multiplet structure of peak *H* is resolved by fixing the intensity ratio of the $1s^{-2}2p^{-1}(^2P)\rightarrow 1s^{-1}2p^{-2}(^2P)$ and $1s^{-2}2p^{-1}(^2P)\rightarrow 1s^{-1}2p^{-2}(^2D)$ transitions (9:5) using theoretical values of Lahtinen and Keski-Rahkonen.[11]

Table II compiles the influence of the electron-impact energy on the intensity $K\alpha_s^h$ relative to $K\alpha_2^h$. Since the uncertainties of some of the lines are fairly large especially at higher electron-impact energies, it becomes difficult to extract a general behavior. Therefore, a straight line fit $y=a+bE_0$, where E_0 denotes the electron-impact energy, was made to the individual intensities at various impact energies. The results of *a* and *b* are also listed in Table II and their implications will be discussed in Sec. IV.

In Table III the observed intensity ratios of the hypersatellite to $K\alpha$ intensity, $I(K\alpha_2^h)/I(K\alpha)$, are listed at various impact energies. Applying the appropriate corrections for the crystal reflectivity, the detector efficiency at the two different x-ray energies, and using the fluorescence yield $\omega(K\alpha_2^h)/\omega_K=1.11$—as obtained from the theoretical calculations for Ne (Ref. 21)—we deduce the cross-section ratios listed in column 2. The third column contains the theoretical *K*-shell single-ionization cross section by Scofield extrapolated to Na according to a procedure which will be described in detail elsewhere.[22] The validity of the extrapolation procedure was checked using the available experimental data for the neighboring elements $Z=8$ and $Z=10$. The present σ_K values are close to those predicted by the scaling behavior proposed by Drawin.[23,24] The last column exhibits the deduced double *K*-shell ionization cross section of sodium.

IV. DISCUSSION

A. Hypersatellite energies

A scrutiny of Table I reveals that the observed energies for the designated transitions are quite close to those ob-

TABLE II. Intensities of the designated spectral transitions of sodium relative to the $K\alpha_2^h(L^0)$ hypersatellite at various impact energies.

	Designated transition		Impact energy (keV) 15	25	50	100	150	200	*a*	*b*
G	$K\alpha_2^h(L^0)$		100.0±5.2	100.0±8.1	100.0±8.5	100.0±10.0	100.0±16.2	100.0±17.3		
		$^2P\rightarrow{}^2P$	36.3±2.5	46.7±3.6	29.9±5.2	74.3±7.1	43.8±11.1	46.4±11.6	37±7	0.13±0.12
H	$K\alpha_2^h(L^{-1})$									
		$^2P\rightarrow{}^2D$	20.3±1.4	26.1±2.0	16.8±3.0	41.6±4.0	24.5±6.2	25.9±6.4	20±4	0.07±0.07
I	$K\alpha_2^h(L^{-2})$		24.3±1.6	40.9±3.4	37.6±8.8	7.2±9.2	37.3±15.9	81.9±17.4	25±5	0.17±0.11
J	$K\alpha_2^h(L^{-3})$		11.0±4.9	42.4±3.6	21.1±7.7	29.4±9.1	34.9±16.1	80.7±17.8	18±10	0.20±0.15
K	$K\alpha_2^h(L^{-4})$		20.9±4.9	86.6±8.1	46.4±8.1	54.9±9.6	31.1±16.6	89.7±17.7	35±17	0.20±0.25
L	$K\alpha_2^h(L^{-5})$		31.9±5.0							

TABLE III. Double-ionization cross section of sodium of various electron-impact energies.

Impact energy (keV)	$10^{+4}\, I(K\alpha_2^h)/I(K\alpha)$	$10^{+4}\, \sigma_{K-2}/\sigma_K$	σ_K[a] (10^{-28} m^2)	σ_{K-2} (10^{-28} m^2)
15	3.96±0.33	3.05±0.25	177 63	5.42±0.45
25	3.20±0.39	2.46±0.30	122 42	3.01±0.37
50	3.49±0.43	2.68±0.33	7419	1.98±0.24
100	4.75±0.72	3.65±0.55	4672	1.71±0.26
150	3.94±0.71	3.03±0.55	3689	1.12±0.20
200	5.02±2.51	3.86±1.93	3190	1.23±0.61

[a] K-shell ionization cross section obtained by extrapolation of the theoretical values by Scofield (Ref. 22).

tained in previous measurements of Lahtinen and Keski-Rahkonen in electron excitation[11] and of Watson *et al.* in heavy-ion collision[17] for the corresponding transitions. The present values are also quite close to the theoretically calculated values, using a Hartree-Fock and Dirac-Fock program,[17] for hypersatellite and its satellites. This validates our assignment of peaks in the sodium spectrum. It is interesting to see that for $K\alpha_2^h(L^{-5})$ the experimental energy is some 8—10 eV less than the theoretically predicted value. A similar observation was also made by Watson *et al.*[17] for Na in heavy-ion collisions. Benka *et al.*[25] observed the same trend for fluorine when theoretical predicted energies were found to be higher than the experimentally observed transition energies. Watson *et al.*[17] have attributed it to the rapid electron transfer to $n>2$ levels of sodium following multiple ionization and prior to K x-ray emission. The increased screening due to electrons in the outer shells ($n>2$) would suppress the hypersatellite energy. The same mechanism of rapid electron transfer seems plausible in the present experiment.

B. Intensities and cross sections

The $K\alpha^h$ transition recorded in the present experiment corresponds to the $K\alpha_2^h$ transition since the $K\alpha_1^h$ transition is suppressed according to the L-S electron-electron coupling scheme where the $1s^{-2}(^1S_0)\rightarrow 1s^{-1}2p^{-1}(^3P_1)$ ($K\alpha_1^h$) spin-flip transition is strictly forbidden. The detection of a $K\alpha^h$ transition is made possible from chlorine,[26] where the deviation from L-S coupling is appreciable and it thus could be considered as the starting element for the intermediate coupling.

Table II compiles the intensity of various $K\alpha_s^h$ transitions relative to $K\alpha_2^h$ intensity for different impact energies. Before entering the discussion on the behavior of these transitions with electron-impact energies, we would first like to focus attention on the dependence of the K-shell electron double-ionization cross section of the electron-impact energy. From Table III it becomes evident that the double-ionization cross section decreases roughly by a factor of 4 with the change in electron-impact energy from 15 to 200 keV. A previous measurement of Lahtinen and Keski-Rahkonen[11] on the K-shell electron double-ionization cross section of sodium is available in the literature with a small electron-impact-energy overlap (15—25 keV) with the present experiment. Both experiments are at variance with each other by about a factor of 2 in this region. The origin for this discrepancy is not evident since two different experimental setups have been employed. It is worthwhile to mention that in Ref. 11 the thin sodium target had a thick substrate of aluminum and a sophisticated procedure had to be adopted to rectify the substrate effect. A comparison of the measured values of the K-shell double-ionization cross section with theoretical predictions is compiled in Table IV, where the values of Refs. 11—13 have been extracted from Fig. 4 of Ref. 11. The agreement between our measurement and the classical[12] as well as quantum mechanical[13] calculation is satisfactory.

It should be noted, however, that the energy dependence of the double-ionization cross section, as found in the present work, is in better agreement with the former experiment,[11] than with the theoretical prediction.[12,13] Fitting a power law of the form $\sigma_{K-2}=aE_0^b$, where a and b are constants and E_0 is the electron bombarding energy, to the present data in the energy range $15\leq E_0\leq 200$ keV as well as to the values of Ref. 11 for $9\leq E_0\leq 25$ keV—the data points have been taken from the figure—we obtain $b=-0.6$ and -0.4, respectively. The classical and the quantum mechanical calculations yield $b=-1.4$ and -1.3, respectively. The difference between experiment

TABLE IV. A comparison of experiment and theory for the K-shell electron double-ionization cross section at 15 and 25 keV (in 10^{-28} m^2).

Impact energy (keV)	Experiment		Theory	
	Present work	Ref. 11[a]	Ref. 12[a]	Ref. 13[a]
15	5.42±0.45	10.7	6.9	8.5
25	3.01±0.37	9.5	3.3	4.2

[a]Values have been obtained from Figs. 3 and 4 in Ref. 11.

and theory may be caused by the fact that both theoretical approaches are nonrelativistic which naturally yields a faster decrease of the cross section with increasing impact energy, since relativistic effects, which cause a rise of the cross section,[27] are not taken into account. For the single-ionization cross section of Na, we deduce from the extrapolated relativistic calculation by Scofield[22,28] a value $b=-0.7$, which exhibits a swifter decrease of the cross section in the energy region of present interest than predicted by nonrelativistic theories.

In conclusion, we state that the observed energy dependence of the double K-shell ionization cross section contradicts the proposition by Watson *et al.*[17] that the main process of multiple ionization is a shake-off process, which is energy independent. The strong contribution of an impact-energy-dependent binary-encounter process in the multiple-excitation mechanism is also evident in the previous work on $K\alpha$ satellites[16,29] and is in support of the present findings.

Finally, we return to the compilation of the $K\alpha_s^h$ transitions listed in Table II. The fit of a straight line to the intensities, as described above, reveals that the transitions H through G show more or less the same electron-impact energy dependence as the hypersatellite line (G), since the values of the slopes vanish—with the exception of I and J—within the quoted error limits. Since a possible systematical error caused by the background subtraction is not yet included, even the small values of b for lines I and J are probably comparable with zero. Thus the $K\alpha_s^h$ transitions are also strongly energy dependent. Finally, it is noted that the comparable intensity of several $K\alpha_s^h$ to $K\alpha_2^h$ transitions contradicts the previous belief that the electron-impact ionization usually creates only pure K^{-2} states and only very little $K^{-2}L^{-n}$ ($n>1$) states.[4,30]

C. Natural linewidth of the hypersatellite line

The inspection of Figs. 2 and 4, respectively, reveals that the width of the hypersatellite line (G) is clearly larger than that of the $K\alpha$ line. Since the overall resolution of a line depends on the aperture of the Soller slits, the finite width of the rocking curve of the crystal, and the natural linewidth, one can deduce the natural linewidth corresponding to the $K\alpha_2^h$ transition. The observed linewidth of the $K\alpha$ line amounts to $\Gamma=3.1$ eV. Assuming a natural linewidth of $\Gamma_K=0.3$ eV (Ref. 31), a deconvolution of these two distributions yields the instrumental width $\Gamma_I=2.95$ eV, where Gaussians have been used to describe the different lines. This instrumental width is angle and, therefore, energy dependent, as can be seen from the Bragg condition. For the TlAP crystal this instrumental width increases by about 11% (i.e., $\Gamma_I^h=3.28$ eV) for the necessary change of angle from the $K\alpha$ to the hypersatellite transition.[15] By deconvolution of the instrumental distribution Γ_I^h with the distribution of the observed total width of 4.6 eV, the natural width of the $K\alpha_2^h$ hypersatellite line (G) is obtained to be 2.2 ± 0.4 eV. This is an increase of the natural width of a hypersatellite line by about a factor of 6 to 8 as compared to the natural width of a $K\alpha$ line. This indicates a drastic reduction of the lifetime of a double K vacancy state to $0.3\times10^{-15}s$ from a value of $2.2\times10^{-15}s$ for the single K vacancy state. It should be noted, finally, that the explanation by Mossé *et al.*[32] is not supported in the present work. According to these authors, the total width of the hypersatellite as observed for Cu is given by the expression $3\Gamma_K+\Gamma_L$. For the present case, however, $3\Gamma_K+\Gamma_L$ amounts in the case of Na to about $\Gamma=0.9$ eV as compared with the deduced value of 2.2 ± 0.4 eV.

V. CONCLUSION

The energies of the $K\alpha$ hypersatellite ($K\alpha_2^h$) and its satellites ($K\alpha_s^h$) are measured with high accuracy. The experimental energies corroborate the theoretical prediction except for a deviation of some 8–10 eV for the $K\alpha_2^h(L^{-5})$ line. This deviation may be attributed to the rapid electron transfer to $n>2$ shells following multiple ionization. The relative intensities of $K\alpha_s^h$ were found to be dependent on the electron-impact energy which indicates that the excitation mechanism of atoms is energy dependent and is not a pure shake-off.

The intensity comparison of $K\alpha_s^h$ with $K\alpha_2^h$ lines indicates that, even in electron-atom scattering, the excitation of $K^{-2}L^{-n}$ ($n>1,\ldots,5$) states is equally as prominent as the excitation of a pure K^{-2} state. Furthermore, the present experiment furnishes new values of the electron double-ionization cross section which are comparatively closer to the theoretical predictions. Finally, the natural linewidth of the hypersatellite lines exhibits an increase of a factor of 7 as compared to the $K\alpha$ linewidth.

ACKNOWLEDGMENTS

We would like to thank H. Folger (Gesellschaft für Schwerionenforschung Darmstadt m.b.H.) for furnishing the targets. One of us (A.K.) is thankful to the Alexander von Humboldt Foundation for partial financial support of the present work. This work was also supported by Deutsche Forschungsgemeinschaft.

*Present address: California State University, Long Beach, CA 90840.

[1]J. P. Briand, P. Chevallier, M. Tavernier, and J. P. Rozet, Phys. Rev. Lett. **27**, 777 (1971).

[2]S. I. Salem and A. Kumar, Phys. Rev. A **28**, 2245 (1983).

[3]D. J. Nagel, A. R. Knudson, and P. G. Burkhalter, J. Phys. B **8**, 2779 (1975).

[4]O. Keski-Rahkonen, J. Saijonmaa, M. Suvanen, and A. Servomaa, Phys. Scr. **16**, 105 (1977).

[5]P. Richard, W. Hodge, and C. F. Moore, Phys. Rev. Lett. **29**, 393 (1972).

[6]T. Åberg and M. Suvanen, in *Advances in X-Ray Spectroscopy*, edited by C. Bonnelle and C. Mande (Pergamon, New York, 1980).

[7]V. Horvat and K. Ilakovac, Phys. Rev. A **31**, 1543 (1985).
[8]N. Cue, W. Scholz, and A. Li-Scholz, Phys. Lett. **63A**, 54 (1977).
[9]P. Richard, in *Atomic Inner-Shell Processes*, edited by B. Crasemann (Academic, New York, 1975), p. 73.
[10]M. H. Chen, B. Crasemann, and H. Mark, Phys. Rev. A **25**, 391 (1982).
[11]J. Lahtinen and O. Keski-Rahkonen, Phys. Scr. **27**, 334 (1983).
[12]M. Gryzinski, Phys. Rev. **138**, 336 (1965).
[13]J. Saijonmaa, Phys. Scr. **17**, 457 (1978).
[14]T. Grundey, H. Heinrichs, U. Klein, G. Müller, G. Nissen, H. Piel, H. Genz, H.-D. Gräf, M. Janke, A. Richter, M. Schanz, E. Spamer, and O. Titze, Nucl. Instrum. Methods **224**, 5 (1984).
[15]S. Reusch, H. Genz, W. Löw, and A. Richter, Z. Phys. D **3**, 379 (1986).
[16]W. Löw, H. Genz, A. Richter, and K. G. Dyall, Phys. Lett. **100A**, 130 (1984).
[17]R. L. Watson, B. B. Bandong, J. M. Sanders, and K. Parthasaradhi, Phys. Scr. **31**, 184 (1985).
[18]H. Genz, A. Kumar, W. Löw, and A. Richter (to be published).
[19]C. Froese-Fischer, Comput. Phys. Commun. **1**, 151 (1969).
[20]P. Desclaux, Comput. Phys. Commun. **9**, 31 (1975).
[21]C. P. Bhalla, J. Phys. B **8**, 1200 (1975); **8**, 2787 (1975).
[22]C. Jakoby, H. Genz, and A. Richter (unpublished).
[23]H.-W. Drawin, Z. Phys. **164**, 513 (1961).
[24]J. Jessenberger and W. Hink, Z. Phys. A **275**, 331 (1975).
[25]O. Benka, R. L. Watson, B. Bandong, and K. Parthasaradhi, Phys. Rev. A **29**, 123 (1984).
[26]C. F. Moore and H. Wolter, J. Phys. **6**, L124 (1973).
[27]H. Genz, Comments At. Mol. Phys. **14**, 173 (1984).
[28]J. H. Scofield, Phys. Rev. A **18**, 963 (1978).
[29]N. Cue and W. Scholz, Phys. Rev. Lett. **32**, 1397 (1974).
[30]E. Mikkola and J. Ahopelto, Phys. Scr. **27**, 297 (1983).
[31]V. O. Kostroun, M. H. Chen, and B. Crasemann, Phys. Rev. A **3**, 533 (1971).
[32]J. P. Mossé, P. Chevallier, and J. P. Briand, Z. Phys. A **322**, 207 (1985).